Assessment of robustness of structures: current state of research

STRUCTURAL RESPONSE TO HIGH IMPULSIVE LOADS: DYNAMIC EFFECTS AND ANALYSIS APPROACHES

YONG LU

Institute for Infrastructure and Environment, School of Engineering, The University of Edinburgh
The King's Buildings, Edinburgh EH9 3JL, UK
Email: yong.lu@ed.ac.uk

Abstract

Structural response to high impulsive loads such as impact and blast involves a series of dynamic effects of distinctive characteristics. These vary from the high intensity, high strain rate effect at the material level; various dynamic modes and failure mechanisms at the structural component level; to the dynamic amplification associated with the transition to a typical double-span mechanism in the process of the progressive collapse due to a sudden removal of vertical load carrying member(s). This paper discusses the characteristics of these different dynamic effects and introduces some associated research studies. The governing mechanisms in the different regimes of dynamic effects are highlighted and appropriate analytical and numerical modelling approaches are discussed.

Keywords: dynamic effects, blast, failure modes

1. Introduction

Impulsive loads such as blast and impact are important factors in the protective design of defence and critical civil engineering structures. When a structure is subjected to this type of high-peak and short-duration loads, the response may be generally divided into three phases according to the underlying dynamic processes, namely, 1) shock and stress wave phase within the body of material in the structural members directly acted upon by the shock load, 2) shear and bending deformation of the structural members due to the energy imparted by the load impulse, and 3) system level response as a result of disruption of the gravity load path due to a sudden loss of one or more of the directly affected components, leading possibly to a progressive collapse.

The above three phases are generally sequential in time but each has a distinctive time scale, and the dynamic effects and governing mechanism differ. Generally speaking, Phase-1 can be a sub-millisecond process, in which the material could be subject to very high strain rate, and hence the response and damage is dictated by the material responses. Phase-2 involves the dynamic response of a structural member; various modes of failure may occur depending upon the duration of the load, which may be translated as the dominant frequency of the load pulse. Phase-3 is actually an indirect effect, and its dynamic process is virtually independent of the initiating shock load.

Extensive studies in the literature on the general subject of impact and blast effects may also be broadly classified along the line of the above mentioned three response categories, namely i) dynamic response of materials, in particular concrete, and fracture and fragmentation [e.g., Brace and Jones, 1973; Li and Meng, 2003; Lu and Xu, 2004; Lu and Tu, 2008]; ii) effect of blast load on structural members, typically RC columns and slabs [e.g., Krauthammer et al., 1993; Lellep and Torn, 2005; Gong and Lu, 2007; Ma et al. 2007], and iii) progressive

collapse of a large portion or the entire structural system.

This paper will examine the dynamic processes involved in the three response phases and the associated characteristics in the different dynamic regimes, especially concerning concrete structures. A series of studies conducted by the author and his co-workers on the related topics will be described, including studies on the strain rate effect on concrete materials using a mesoscale modelling approach, and a Timoshenko beam-based nonlinear model for the analysis of beam-column members with incorporation of global participation under shock and blast loads. The dynamic effect during the transient phase of a sudden removal of a column on the double-span mechanism and the corresponding demands on the resistance and deformation capacities will also be discussed.

2. Characteristics of Impulsive Loads and Structural Responses

Most of the shock and impact loads may be characterized by a pulse action, in a simple fashion a triangle pattern as shown in Fig. 1(a). It has a high peak load *P* (normally order of MPa in terms of pressure) and a short duration (normally order of milliseconds). The area covered under the load curve gives rise the impulse *I*. It is effectively the relative magnitude of the peak load versus the impulse (hence the duration) that determines the dynamic effect of such an impulsive load, as schematically illustrated with a pressure-impulse (*P*-*I*) diagram in Fig. 1(b).

It is generally established through theoretical and experimental studies that, as the duration becomes shorter, the dynamic effect tends to be shock wave governed and the material undergoes stress wave as it propagates and reverberates within the boundary of the component (shown as regime I). The material could be breached in the form of crushing and spalling without a significant participation of the member level response in terms of deflection, shear and bending. On the other hand, an impulsive load with a modest peak load but large impulse, i.e. a "longer" duration, will tend to induce a quasi-static type of global response involving bending as well as shear (shown as regime IV). In-between these two extreme scenarios will be a varying degree of mixed modes of responses, including a mixed stress wave and direct shear (II), and a mixed diagonal shear and bending (III).

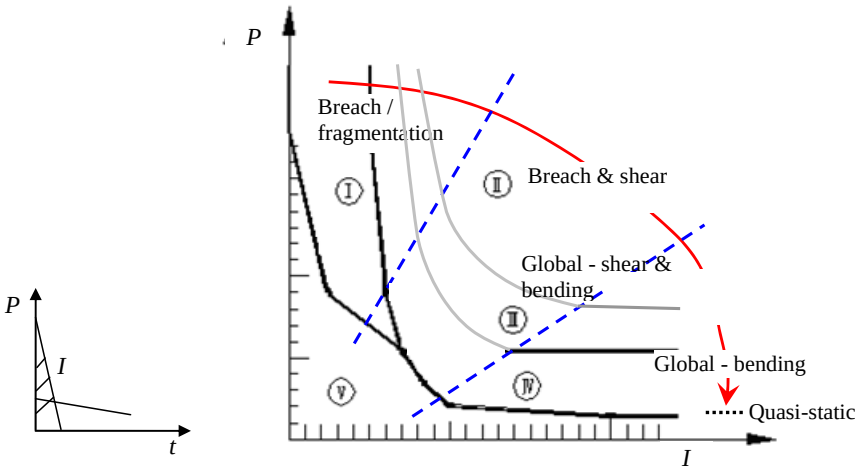

Fig. 1. Schematic of (a) impulsive load, and (b) P-I diagram with variation of response-failure modes

For regime I, and to some extend regime II, the loading effect is dominated by the dynamic response of the bulk material, and the problem effectively falls into a continuum domain, for which an appropriate high-fidelity finite element model or equivalent would be required. For responses in the regimes of III and IV, a beam-column approach with adequate representation of the shear deformation will be suitable to capture the primary dynamic effects. As a matter of fact, in the situation where the response is dominated by the shear and bending at the member level, a beam-column based solution can be a more robust approach as it allows the resistance functions and hysteretic rules governing the shear and flexural behaviour to be defined directly. This is desirable in view of the fact that it is still a challenging task for a general FE model to fully reproduce such behaviours in reinforced concrete members, especially when a dynamic cyclic process is involved.

3. Dynamic Effect at Material Level: Understanding the Strain Rate Effect

As indicated in Fig. 1, for impulsive loads falling into the very high peak-very short duration regime, local material failure could prevail due to a rapid buildup of stresses and the stress waves, leading to breaching of the material in a form of crushing and/or spalling before any appreciable shear or bending deformations come into play. A typical such damage pattern is shown in Fig. 2(a). Similar damage can be expected from other high impulsive loads such as high velocity impact. The response in this regime is primarily governed by the material dynamic behaviour, for which the strain rate effect is a pertinent subject. Fig. 2(b) shows some selected numerical simulations [e.g. Xu and Lu, 2006] for this range of the dynamic effects.

(a) Local damage of RC due to close-in blast [Gebbeken, 2006]

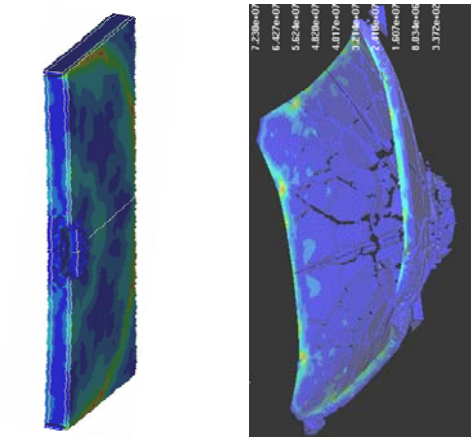

(b) Simulated local damage (spalling) and break-up of concrete component

Fig. 2. Dynamic effects governed by stress wave and dynamic behavior of material

Whereas the strain rate effect for metals is generally well understood, the mechanisms underlying the experimentally apparent strain rate enhancement of the strength of quasi-brittle materials, in particular concrete, have been a subject of continued securitisation and debate over the last three decades or so. The general consensus tends to emerge in more recent years, such that the dynamic increase factor (DIF) for concrete in compression is largely due to the dynamic structural effect within a sample or representative size of the bulk material, whereas the DIF for concrete in tension can only be attributed to processes at the micro-mechanical level rather than any bulk dynamic effect. These observations have significant implications in the correct consideration of the strain rate effect or DIF in the modeling and analysis of concrete structures subjected to high impulsive loading. In particular, in case a refined model is formulated in such a way that the bulk dynamic (inertia) effect is well represented, any DIF at the material constitutive property level for compression should reasonably be voided to avoid "double counting", while the DIF for tension needs to remain.

In the sub-sections that follow, the dynamic behaviour of concrete material will be discussed in light of a few recent studies using a meso-scale concrete model. In addition to the well-known inertia confinement effect under compression, the contribution of the mesoscopic heterogeneity, and the effect of propagating failure under very high strain rate compression will be highlighted.

3.1. *Mesoscale Model for Dynamic Response of Concrete*

Concrete is by nature a heterogeneous material with coarse aggregates embedded in the mortar matrix. The bulk behaviour of concrete is deemed to become stabilised in a sample size (or a representative volume within a structure) of at least a few times of the maximum aggregate particle size and under a reasonably uniform stress distribution. This requirement is implicit in the homogenization treatment of concrete in a conventional analysis. However, under shock and blast loading, stress waves propagate in the material with a drastic spatial and temporal variation. The stress-strain gradient can be very large such that the heterogeneities in concrete become significantly involved in influencing the bulk material behaviour. While homogenisation may still be acceptable concerning the global behaviour at a component or structural level, it is obviously inadequate for probing into the mechanisms underlying the dynamic behaviour of concrete at high strain rates where sub-scale processes play an important role. As such, a mesoscale modeling approach is deemed to be appropriate and necessary.

At the mesoscopic level, concrete manifests as a composite comprising of three distinctive phases, namely, coarse aggregate, mortar matrix and interfacial transition zone (ITZ). Mesoscale model of concrete has been a subject of considerable interest in the quasi-static modelling literature of concrete material. Three main alternative approaches exist, namely lattice models [e.g. Wittmann et al., 1984; Schlangen & van Mier, 1992; Man and van Mier, 2008]; discrete element and discrete particle models [e.g. Cundall and Strack, 1979; Donze et al., 1999; Cusatis et al., 2003] and continuum-based FE models [e.g. Wang et al. 1999, Wriggers and Moftah, 2006]. A key challenge associated with the lattice models is the difficulty in determining the equivalent model parameters. Similar issues exist in the DEM approach where the virtually continuous interface between aggregates and the mortar matrix (at least up to a moderate nonlinear response stage) is represented through artificial local contacts. The determination of the modelling parameters in a continuum-based FE model, on the other hand, is seemingly more straightforward. In more recent years, the mesoscale modelling approach has been increasingly used in the study of the dynamic behaviour of

concrete, mostly using simplified mesoscale structure such as spherical aggregates [e.g. Zhou and Hao, 2008].

To represent in a more realistic manner the meso-structure of concrete while allowing for dynamic analysis under complex stress conditions, a comprehensive mesoscale modelling framework has been developed. The framework encompasses the generation of random mesoscale geometry in 2D as well as 3D, creation of the multi-layer FE model, and the subsequent dynamic analysis performed using a general dynamic analysis solver (herein using LS-DYNA) [Lu and Tu, 2008; Tu and Lu, 2011]. Fig. 3 depicts a typical 2D mesoscale geometry model and the corresponding FE mesh. Two alternative schemes may be considered to represent the ITZ, using either the classical cohesive interface elements, or an equivalent layer of solid elements. Material models with rate adjustable features, such as the Concrete Damage model or K&C model [Malvar et al., 1997], can be readily employed to represent the constituent materials in the mesoscale model to facilitate comprehensive analysis under high rate and high pressure dynamic loading.

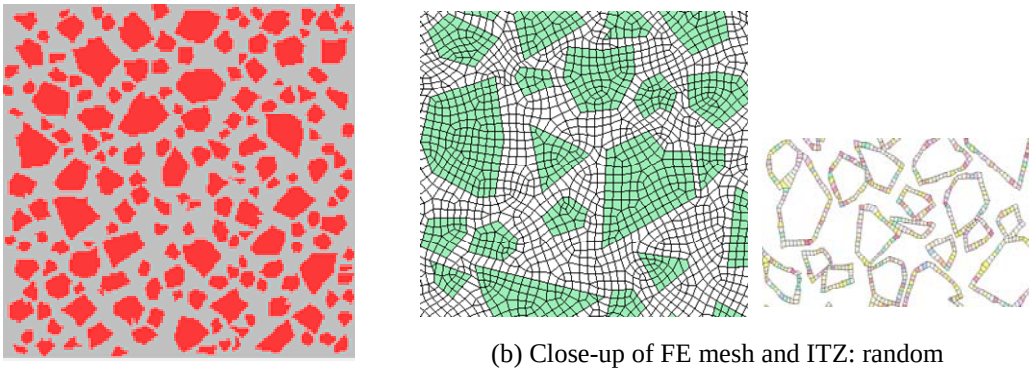

(a) Sample meso-geometry

(b) Close-up of FE mesh and ITZ: random properties possible within each phase

Fig. 3. 2-D Random mesoscale structure of concrete and FE mesh

Fig. 4. shows a full 3D mesoscale model with random aggregates, including the FE mesh and an example analysis for a sample specimen under compression [Song and Lu, 2010]. As can be expected, the computational cost for generating and running such a full 3D mesoscale analysis is rather costly. The following discussion will be based on the analysis using the 2D and a “pseudo 3D” mesoscale model. The general concept and the effect of the pseudo 3D model in withholding a 3-D stress environment in a dynamic response while maintaining the essential mesoscale feature is illustrated in Fig. 5. More details about the pseudo-3D model can be found in Lu et al. [2010].

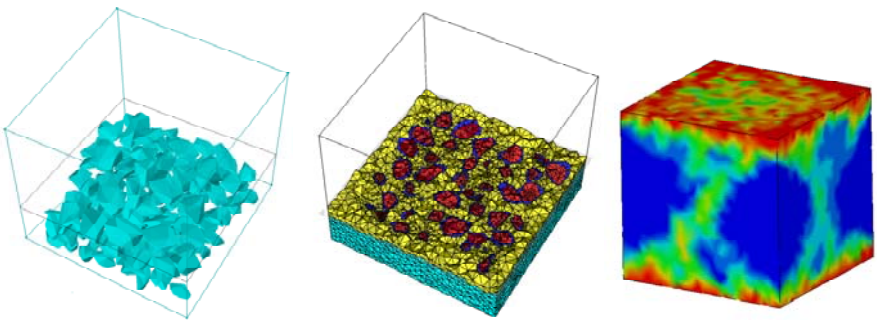

Fig. 4. A full 3-D random mesoscale FE model of concrete

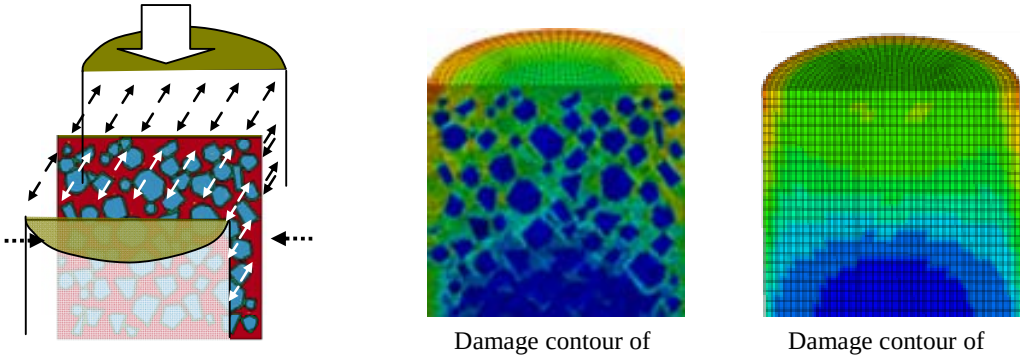

Fig. 5. Concept of a pseudo-3D mesoscale configuration and its effect in preserving realistic 3-D stress environment for the mesoscale plane

3.2. *General Dynamic Behaviour of Concrete under Compression*

Under a quasi-static loading, a sample of concrete material will undergo a process of fracture initiation, growth and coalescence, and major cracks generally develop along the weakest paths, as depicted in Fig. 6(a). When the loading rate is high, however, this pattern of fracture and damage is hindered by the propagating high-intensity stress wave. As a result, damage tends to develop throughout the area affected in a distributed manner, as shown in Fig. 6(b). From such a sharp contrast in the damage and failure processes, it is not difficult to understand the behavioural differences of concrete-like materials under dynamic loading as compared to the quasi-static behaviour.

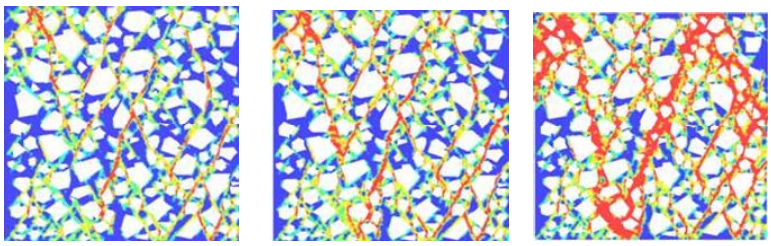

(a) Quasi-static compression without friction on loading faces

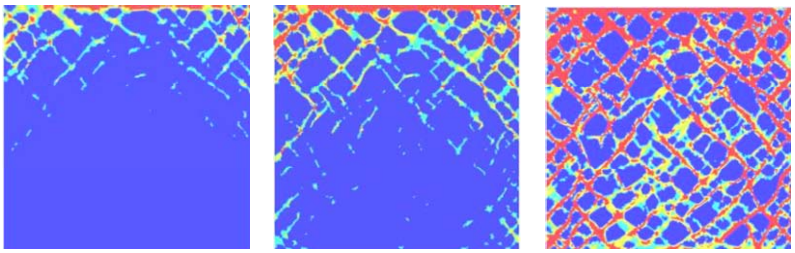

(b) Dynamic compression (nominal strain rate 50 s^{-1})

Fig. 6. Different failure patterns under quasi-static and dynamic compressions

As mentioned earlier, concrete-like materials generally exhibit an increase in the apparent (bulk) strength with the increase of the strain rate. For compression, it is generally understood that the experimentally observed DIF on concrete sample specimens may largely be explained by the inertia confinement effect [e.g. Bischoff and Perry, 1991; Donze et al., 1999; Li and Meng, 2003]. A comparative study using the present mesoscale model and homogenised model in various configurations also demonstrates the same general trend of increase of the DIF with the strain rate without invoking any rate sensitivity in the material constitutive models, as shown in Fig. 7. In addition, the results suggest an appreciable contribution of the mesoscale heterogeneity (i.e. the presence of the stronger aggregates) in the dynamic enhancement of the concrete compressive strength in the high strain rate regime, see Fig. 8. For typical normal concrete with crushed natural aggregates, the contribution of the aggregate strength can account for as much as 20% in the increase of the dynamic strength of the bulk concrete [Song and Lu, 2012].

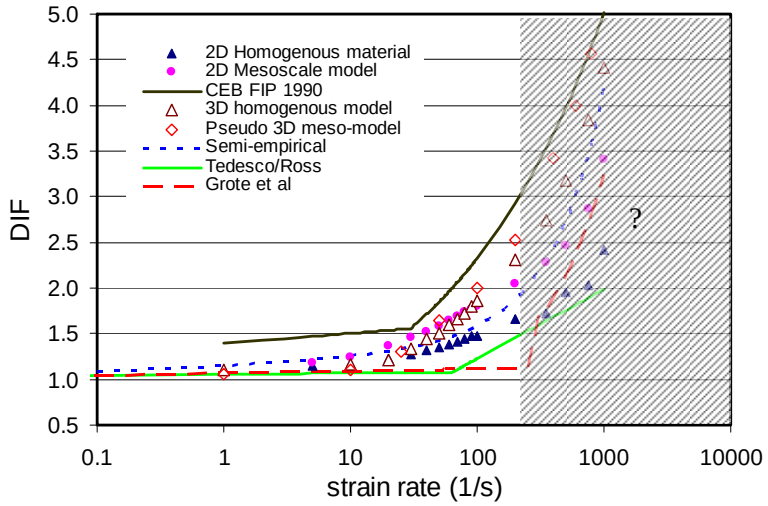

Fig. 7. Compression DIF from numerical experiments comparing to empirical formulas

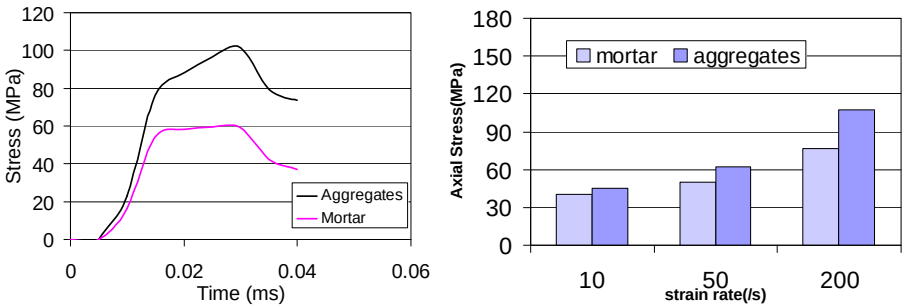

Fig. 8. Variation of peak stresses in mortar and aggregates with increase of strain rate

As the strain rate gets considerably high (e.g. above 100 s^{-1}), various complexities arise in the measurement and interpretation of the dynamic response of concrete sample specimens, rendering the reliability of the experimental data in this regime to be questionable, this is marked in Fig. 7 in the shaded region. Fig. 9 further illustrates a comparison of the stress and strain curves under selected strain rates, where “real” stress-strain curves are those extracted from the material point stress within the sample, while the “engineering” stress-strain curves are those obtained using boundary responses in a similar way as generally done in physical experiments (using a Split Hopkinson Pressure Bar apparatus for example). More detailed discussion on such a phenomenon can be found in Song and Lu [2012]. Notwithstanding the

absolute accuracy of the numerical experiments, the relative comparison between the "real" and "engineering" results highlight the margin of discrepancies that may result from different ways of processing and interpretation of the high strain rate responses.

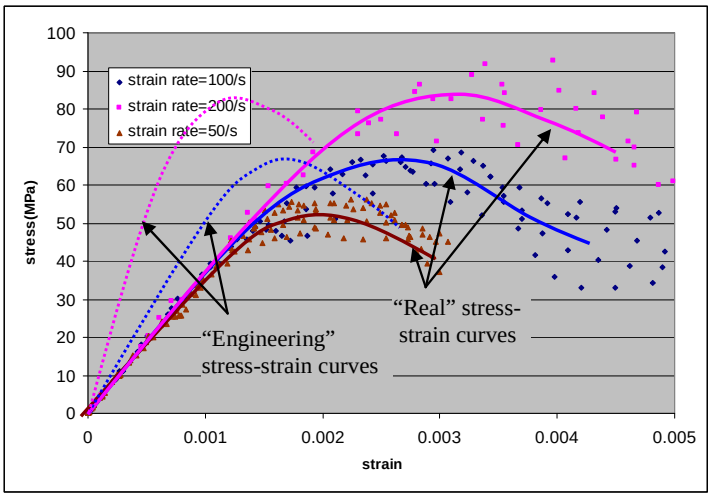

Fig. 9. Characteristics of dynamic stress-strain relationships in high strain rate regime

While the inertia confinement effect can be demonstrated from numerical experiments as a major contributor to the dynamic enhancement of the bulk strength of concrete under compression, such effect cannot explain the increase of the dynamic strength in tension, as demonstrated in a number of numerical studies using various modelling approaches [e.g. Brara et al. 2001; Hentz et al., 2004]. The underlying mechanisms for the dynamic tensile strength increase are believed to originate from the micro-fracture processes and micro-inertia, along with possible contributions from thermo-mechanical and moisture factors. Fig. 10 shows a representative simulation of the tension-spalling response of concrete where a spall test using Hopkinson bar apparatus was modelled using DEM method [Brara et al., 2001].

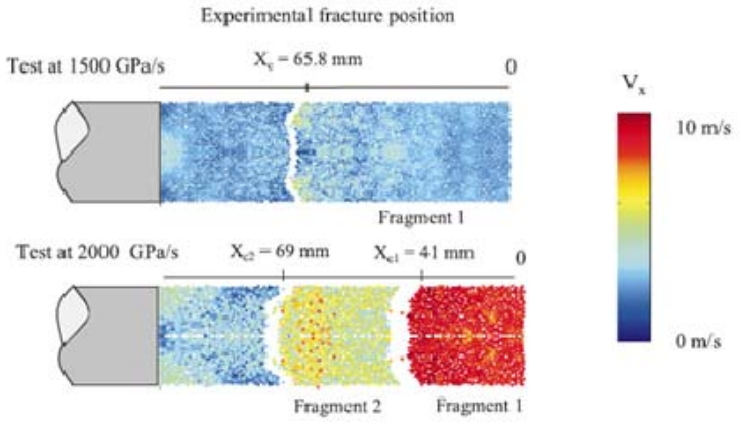

Fig. 10. Numerical simulation of fracture in spalling tests (after Brara et al. [2001])

The mesoscopic heterogeneity can be expected to contribute to a certain extent to the dynamic tensile strength enhancement, as a result of increased involvement of the higher strength aggregates during the course of macro crack formation as a result of rapid buildup of stresses.

This can be confirmed using the present mesoscale model. Fig. 11(a) shows the damage patterns of a spitting tensile loading on a circular disk (Brazilian disk). Comparison of the failure splitting forces (and hence the splitting tensile strength) with the results from the homogeneous models indicate that an increase of order of 20% in the dynamic splitting tensile strength may be attributable to such an effect.

Another related issue to note is the validity of the splitting tensile test in the high strain rate regime. This is essentially a question as to whether a splitting equilibrium similar to a static condition may be established before the onset of the tensile failure. In a dynamic condition this requires a certain amount of time so as to allow a minimum number of stress wave reverberations within the specimen without a premature failure (reaching a critical strain), thus giving rise to a tensile strain rate limit. For normal concrete in a typical splitting disk of 50mm in diameter, the (splitting) tensile strain rate limit can be established around the order of 10 s^{-1}. Further increase of the strain rate will result in the creation of more complex stress fields, as depicted in Fig. 11(b), with no clear splitting tension field along the loading diameter, and consequently the tensile stress can no longer be deduced from the splitting forces.

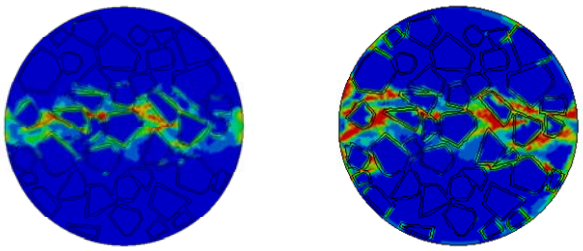

(a) Nominal tensile strain rate = $1s^{-1}$

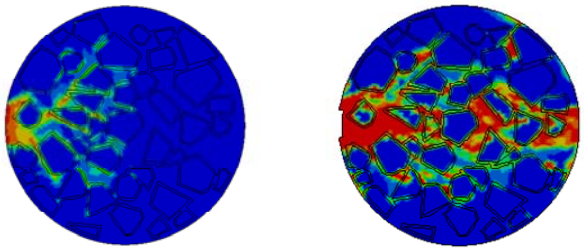

(b) Nominal tensile strain rate = $50s^{-1}$

Fig. 11. Damage patterns under different splitting tensile strain rates

4. Dynamic Effects at Component Level: Shear and Bending Modes of Failure

If the structural member directly acted upon by a blast or impact load does not fail due to breaching from the shock stress wave, it will undergo shear and bending deformation due to the kinetic energy imparted through the impulse-momentum transfer. A simple energy method may be applied to evaluate the maximum response of the structural member, provided the governing response and failure mode can be determined beforehand. Conventional energy method often assumes a bending mode of failure, but in reality the actual governing mechanism will depend on the characteristics of the loading and the dynamic behaviour of the structural member in shear as well as in bending, and a reliable solution may only be obtained

via a rigorous dynamic analysis procedure.

For shear and bending dominated structural member responses, it is neither economical nor necessarily more reliable to use a finite element model; in fact a continuum FE analysis has still only a limited ability in replicating the complex shear resistance mechanisms of a reinforced concrete member. For these reasons, a Timoshenko beam-based model is deemed to be an effective and efficient approach.

4.1. *Overview of the Model Formulation*

Recognizing the fact that the dynamic response of individual beam-columns in a framed structure under impulsive loading may be coupled, to a varying degree, with the response of the structural system, a continuous beam-column model incorporating a point mass at the member end can be envisaged. Such a model is deemed to provide a good representation of the component response and at the same time allows for the contribution from the global system to be accounted for. A model based on these considerations, and taking into account the various possible failure mechanisms, has been developed for the analysis of RC columns subjected to shock and blast load [Gong and Lu, 2007].

The concept of the modelling approach is schematically illustrated in Fig.12. The properties of the critical beam or column in the actual frame are retained in the model, while the participation of the global system in the response of the beam-column member is represented by the addition of a point mass at the member end. The amount of the added point mass is an equivalent quantity which serves to represent the global system effect as if the member being analysed is within the actual frame. As an example, for the analysis of a column under a horizontal impulsive load, the point mass may be approximated by the effective floor mass associated with the particular column.

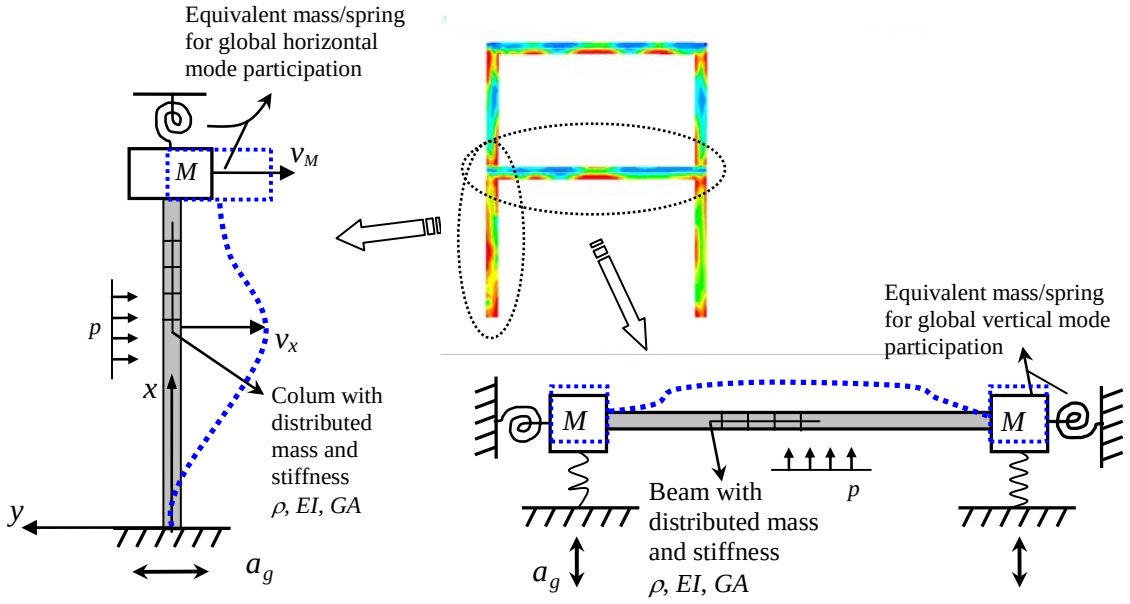

a) Column-Mass-Spring model (horizontal loading)

b) Beam-Mass-Spring model (vertical loading)

Fig. 12. Derivation of beam-column plus lumped mass (M) model for impulsive response analysis

For a generic scenario involving the direct blast load as well as a ground shock, the governing equations of motion may be expressed according to Timoshenko beam theory as:

$$\frac{\partial M}{\partial x} + Q = \rho I \frac{\partial^2 \psi}{\partial t^2} \tag{1}$$

$$\frac{\partial Q}{\partial x} = \rho A\left(a_g + \frac{\partial^2 w}{\partial t^2}\right) - p \tag{2}$$

where:

M , Q = bending moment and shear force, respectively,

I = moment of inertia,

A = cross-sectional area,

ρ = material density,

ψ = rotation of the cross-section due to bending,

w = transverse displacement of the mid-plane of the beam,

a_g = ground shock acceleration, and

p = direct blast load.

For an elastic system with idealised loads (e.g., in the form of a triangle or half-sine pulse), closed-form solutions may be obtained by modal superposition. Fig. 13(a) illustrates the first three modes and the variation of the response of the reduced system with increase of the dominant frequency (or decrease of the duration) of a synthesized high frequency ground shock. Such an elastic solution provides an effective means to explore the possible level of global participation in the column response and the relative importance of the shear and bending mechanisms for a variety of the loads with different dynamic characteristics (i.e. duration or dominant frequencies).

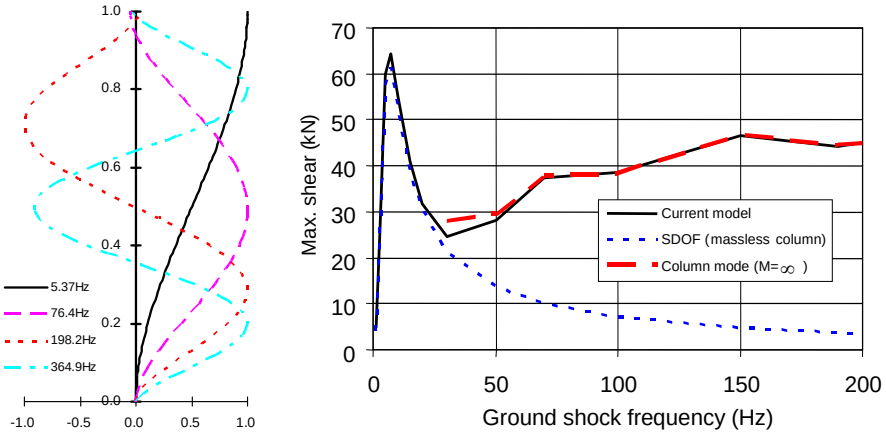

Fig. 13. Representative modes and example elastic response to high frequency ground shock excitation

The nonlinear solution of the dynamic equations can be sought using a finite difference method, provided the resistance functions for the shear and bending responses, as well as the corresponding restoring force (or hysteresis) patterns are available. For an RC beam-column member under shock and blast loading, it has been observed experimentally [Slawson 1984]

that failure is often initiated by direct shear at the supports and occurs shortly after load application; and in some instances diagonal shear failure along the member also developed [Ross, 1983; Hegemier et al., 2002]. Fig. 14 illustrates the failure modes of columns from a field blast test and the associated laboratory simulation tests.

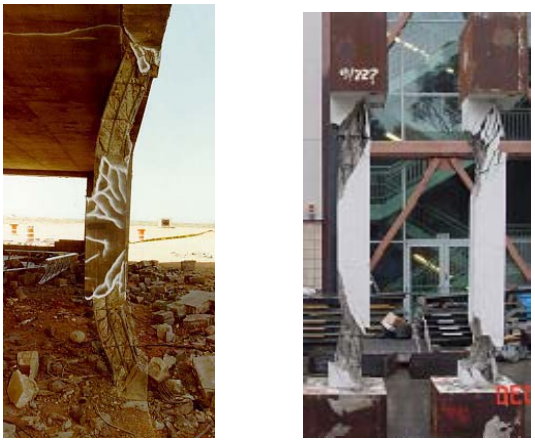

Fig. 14. Field and laboratory-simulated blast tests showing clear shear failure modes in RC columns [Hegemier et al., 2002]

Three basic failure modes may be identified, as illustrated in Fig. 15. While flexural and diagonal shear behaviour of a RC beam-column is a classical topic and standard methods exist for the establishment of their resistance functions (moment-curvature or shear force-shear deformation relationships), relatively less amount of information is available with regard to the direct shear-sliding displacement relationship and the shear behaviour under a very small shear span (e.g., a shear span less than 0.5 times of the cross-section depth). More dedicated studies for such extreme shear behaviour are still required. Moreover, the mechanisms and the extent of the loading rate effect on the shear and bending resistances also warrant special attention.

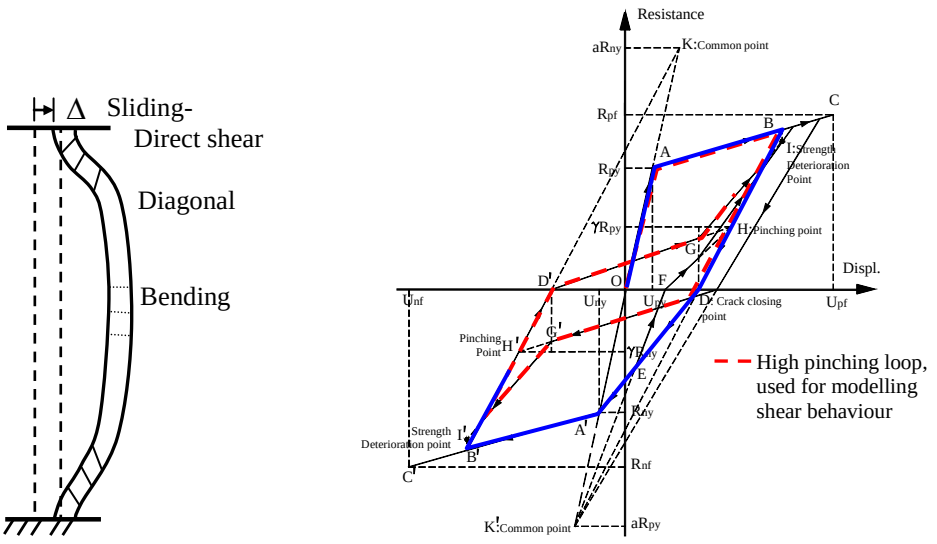

(a) Basic failure mechanisms (b) Generic hysteresis rules

Fig. 15. Schematic of three basic failure mechanisms and restoring force model

For generality in representing a range of possible dynamic responses, a generic three-parameter hysteretic model [Park et al., 1987) is adopted in the current Timoshenko-beam based formulation, as shown in Fig. 15(b). For the flexural nonlinearity, the resistance function is represented herein by a sectional bending-moment vs. curvature relationship, which may be analysed using a standard procedure such as the fibre (or layer) model. The diagonal shear is modelled by the generalised shear force vs. shear strain resistance function, which may be established considering the diagonal shear mechanism using a more detailed analysis, herein using a softened membrane model (SMM) proposed by Hsu and Zhu [2002]. Finally, a direct shear model similar to the one used by Krauthammer [1993] is employed, where an empirical curve comprising three branches bounded by three limit states are considered.

4.2. *Example Analyses*

Fig. 16 illustrates example results using the above model from the analysis of a RC column in three different explosion cases, with a uniform charge weight of 1000 kg TNT but a standoff distance of 10, 20 and 30 m, respectively.

It can be observed that for the first case, which represents a close-range explosion with a scaled standoff of 1 m/kg$^{1/3}$, the response is dominated by excessively high shear deformation near both ends of the column, whereas bending remains in an elastic range. When the distance is increased to 20 m, diagonal shear appears to play a more important role, and large bending deformation also develops at the end regions. Further increasing the distance to 30 m renders the response to be dominated by a bending failure at both ends as well as at in the mid-height, whereas no plastic shear occurs throughout the entire column.

It is also worth noting from the response in the third case that a full cycle with reversed bending takes place, this indicates that the cyclic behaviour could become a sensible factor in the blast response of a RC column in relatively large standoff scenarios.

From the above results as well as an extended parametric study, the following general observations may be drawn:

1) Different ranges of blast loads can cause very different response modes, thus invoking different resistance and failure mechanisms. This has significant implications on the conventional simplified dynamic analysis using a single-degree-of-freedom (SDOF) system, in that both the equivalent SDOF properties (effective mass and effective stiffness) and the resistance functions need be constructed taking full consideration of the different modes of responses. Similarly in a simplified mechanism analysis, care should be exercised so that all possible failure modes are accounted for.

2) For events with a somewhat prolonged duration (blast at a larger standoff for example) the dynamic response may involve appreciable cyclic responses, which would consequently affect the damage state of the structural member and its residual capacities. It should be pointed out that such a cyclic effect is not normally represented in simplified approaches where the maximum responses are of primary interest.

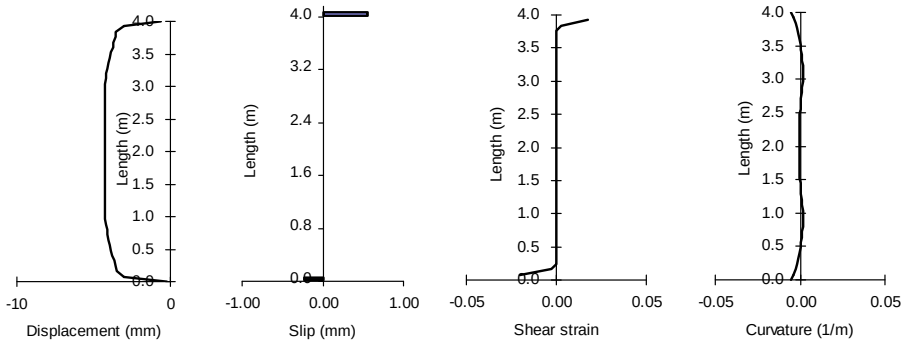

(a) 1000 kg TNT at 10 m standoff

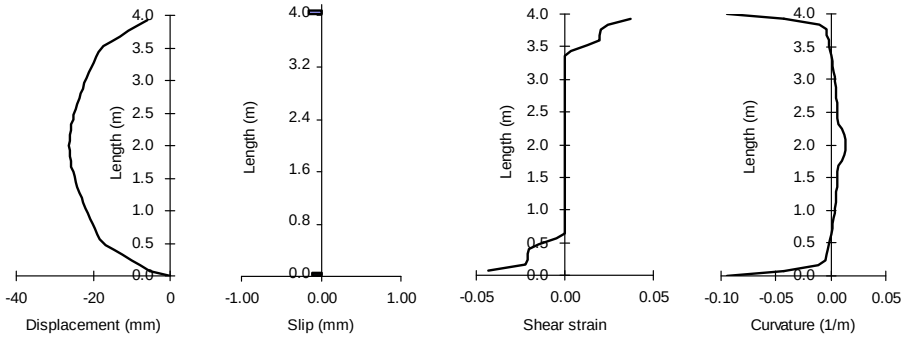

(b) 1000 kg TNT at 20 m standoff

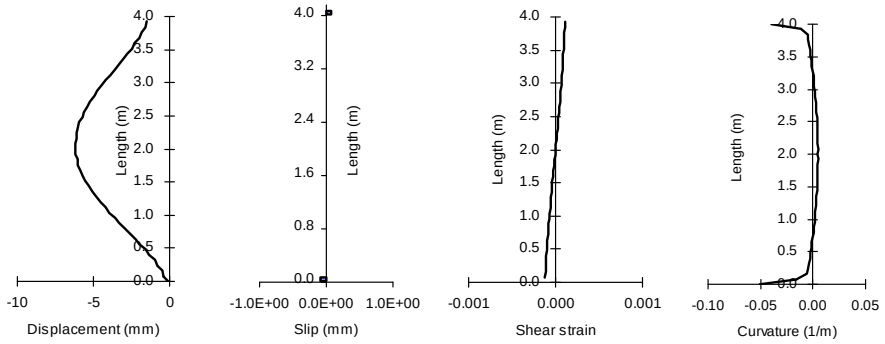

(c) 1000 kg TNT at 30 m standoff

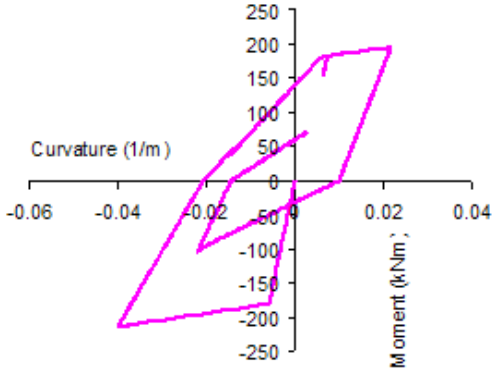

(d) Occurrence of cyclic response for the 30 m standoff case

Fig. 16. Response of a RC column to different blast scenarios

5. Dynamic Effect during Transition to a "Double-span" Mechanism

With the simplified "beam-column plus" model as described in Section 4, the participation of the global dynamic mode on the response of a critical structural member to the direct shock/blast load can readily be analysed. The associated global dynamic response (e.g. the floor movement) can also be assessed from this process. It is worth noting, however, that such a dynamic effect on the global system itself may generally be of secondary importance, especially in near-field blast scenarios as demonstrated from the past experiences and numerical simulation studies [Lu and Wang, 2006].

For the system stability, an indirect transient dynamic effect can be more problematic. As mentioned earlier, if a column is suddenly removed or seriously damaged as a result of the direct impact, the gravity load path is disrupted and if a new equilibrium state can not be established the structure enters into a progressive collapse phase. Despite being a result of gravity load, the transition process with the sudden removal of the vertical member (column) is dynamic, which in turn adds to the demand on the resistance mechanisms against progressive collapse.

A detailed treatment of the topic of progressive collapse is beyond the scope of this paper. Herein we shall focus only on the dynamic effect associated with a sudden removal of a column. For a characterization purpose, the formation of a double-span mechanism in a 2-D frame configuration is considered.

Fig. 17 schematically illustrates a multi-story frame in the event of the removal of an intermediate bottom column. For simplicity, assuming the frame is relatively uniform in elevation, thus the axial force in the remaining columns along the affected column line is insignificant and may be neglected. As such the response in the double-span section of the frame may be represented by the first floor sub-system as shown in Fig. 17(b), with the far ends idealised as fixed at the respective joints.

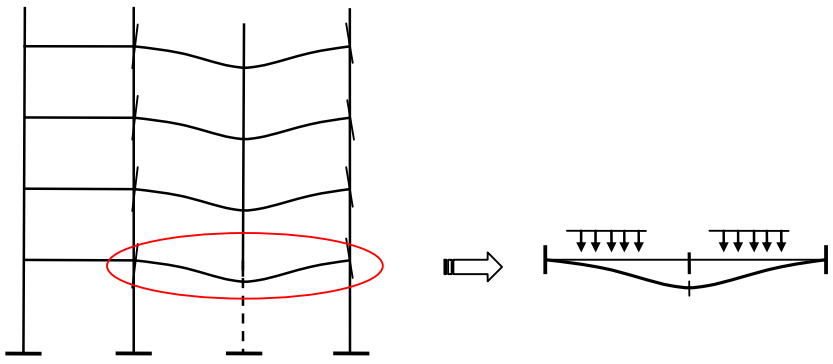

(a) Double-span mechanism in a frame (b) Simplified double-span beam

Fig. 17. Schematic of transition to double-span mechanism due to sudden loss of a column

For a uniformly distributed gravity load *w* on the simplified double-span beam, the dynamic amplification effect assuming an elastic response can be worked out in accordance with the procedure depicted in Fig. 18. The sudden removal of the middle column may be represented by a step load of -N, resulting in a dynamic displacement and hence a force effect with a magnitude being two times of those under a static load -N.

In terms of the bending moments, it is instructive to use the bending moment at the beam end on the original single-span case as a reference, i.e.:

$$M_{1a} = \frac{1}{12} wL^2 = M_{2a} \tag{3}$$

And note also that the bending moments resulting from w being applied on the double-span system without dynamic effect will be:

$$M_{1b,s} = \frac{1}{12} w(2L)^2 = \frac{1}{3} wL^2 \text{ (negative, or hogging moment)} \tag{4a}$$

$$M_{2b,s} = \frac{1}{24} w(2L)^2 = \frac{1}{6} wL^2 \text{ (positive, or sagging moment)} \tag{4b}$$

After combining with the dynamic bending moment due to the step load $-N$, the maximum moments in the double-span beam will be (equivalent to a static effect with -2N = -2wL):

$$M_{1b,d} = \frac{7}{12} wL^2 \text{ (negative moment)} \tag{5a}$$

$$M_{2b,d} = \frac{5}{12} wL^2 \text{ (positive moment)} \tag{5b}$$

where the subscript "*d*" denotes dynamic effect, "*b*" symbolizes the double-span beam as opposed to "*a*" for the intact single-span beams before column removal.

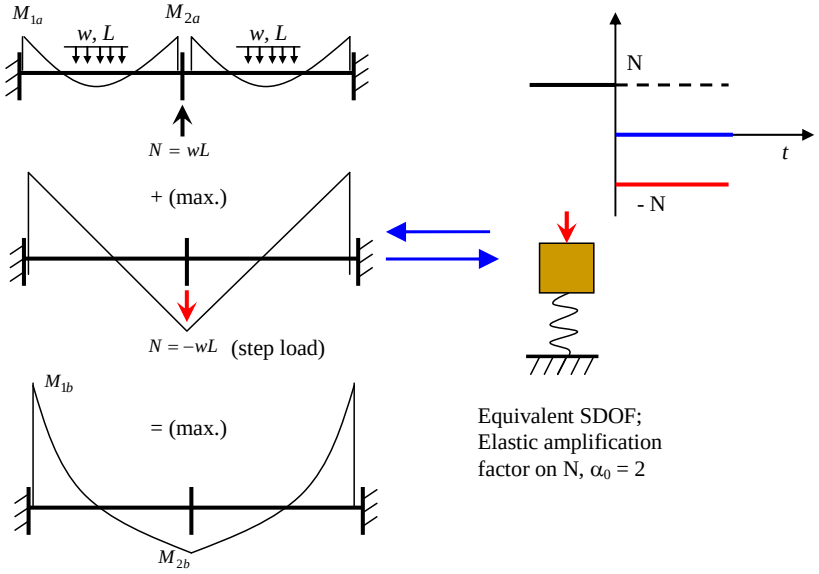

Fig. 18. Dynamic amplification effect on a simplified double-span mechanism

From the above results it can be observed that the dynamic amplification in terms of the bending moment at the support joints of the double-span beam will be 1.75, which is close to the result if the entire gravity load w is treated as a step load (or static equivalent of 2w) on the

double span beam. On the other hand, at the mid-point of the double-span the dynamic moment (positive) is 2.5 times of the static moment (negative). It is worth noting the fact that the sum of the absolute bending moments $M_{1b,d}$ and $M_{2b,d}$,

$$\overline{M}_{b,d} = M_{1b,d} + M_{2b,d} = wL^2 \tag{6}$$

is identical to the sum of the two moments where the gravity load *w* is applied on the double span altogether as a step load. This observation can be useful when it comes to a plastic analysis where re-distribution of the moments can take place.

The above dynamic amplification analysis on the force effects is only valid if the beams possess sufficient strength so that the dynamic demands are within the respective elastic limits. In the simplified scenario herein, this means the moment capacity of the beam at the end joints should be more than 7 times of the original (design) moment effect on the intact spans, not to mention the moment demand in the reversed direction (positive) at the middle joint where the column is removed. In a more rational design scenario, the beams are less likely to possess such a level of the strength capacity reserve, and consequently will develop into inelastic range during the dynamic response. When inelastic response takes place, one can no longer treat the dynamic effect due to the sudden removal of the column by simply amplifying the applied (gravity) load, as the load carrying capacity is already dictated by the available strength; instead an increased plastic deformation will occur. This is analogous to the strength-ductility trade off in seismic response of structures. For an illustrative purpose, herein we assume ideal elastic-plastic system behaviour, and let the ratio between the overall strength capacity and the static demand be:

$$\beta = \frac{\overline{M}_y}{\overline{M}_{b,s}}, \qquad 1.0 \le \beta \le 2.0 \tag{7}$$

Using energy method the following can be obtained:

$$\Delta_d = \frac{1}{2}\frac{\beta^2}{\beta - 1}\Delta_s = \eta\Delta_s \tag{8}$$

where Δ_d and Δ_s represent the dynamic displacement and static displacement of the double-span beam, and η denotes the inelastic dynamic displacement increase factor.

Fig. 19 shows the variation of η with β. It can be seen that as β decreases towards unity, the dynamic (inelastic) displacement increases exponentially.

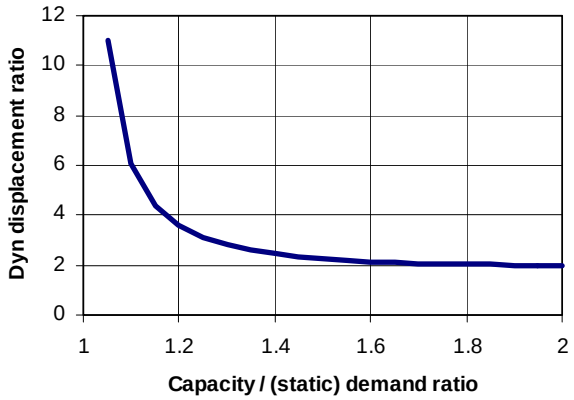

Fig. 19. Amplification on inelastic deformation of the double-span mechanism

At this juncture, it should be noted that as the displacement increases to a certain large magnitude, the resistance mechanism of the double-span beam will start to involve the tension-catenary effect. This could eventually result in a major or even complete shift of the resistance mechanism. Such a change of the resistance mechanism and the associated demand on the joints and critical regions in terms of deformability and ductility are essential topics in the subject of progressive collapse resistance, which however is beyond the scope of the present discussion.

6. Concluding Remarks

Structural response to a high impulsive load, in particular blast and impact, involves a series of distinctive dynamic effects at different response stages; namely, a) transient stress wave effect in the constituent materials of the structure, b) high-frequency dynamic response at structural member level, and c) system transitional dynamic effect due to sudden removal of a loading bearing component. The global dynamic response during the impulsive loading phase, however, is deemed to be of generally secondary importance.

Understanding the different dynamic effects and the governing mechanisms at different stages of the process is essential in the determination of appropriate analysis approaches and effective design counter measures. Whilst a high fidelity numerical model is generally required for the analysis of the stress wave and breaching of materials, where high strain rate occurs, a Timoshenko-beam based method can be a more robust approach for the member level dynamic response analysis.

The transition to a double-span or alike mechanism due to a sudden failure of a vertical load-carrying member involves an indirect dynamic effect. Although in an elastic analysis such a dynamic effect may be represented by an appropriate dynamic amplification of the gravity load acting on the double-span beams, in an inelastic situation such a load amplification is subject to the limit of the available strength. When the strength capacity to the gravity demand ratio reduces towards the lower part of the 1.0~2.0 range, the inelastic deformation will tend to increase exponentially, in which case a tension-catenary mechanism would come into play.

7. References

Bischoff, P.H. and Perry, S.H. [1991] “Compression behaviour of concrete at high strain-rates,” *Mater Struct.* 24, 425-450

Brara, A., Camborde, F., Klepaczko, J.R., Mariotti, C. [2001] “Experimental and numerical study of concrete at high strain rates in tension,” *Mech Mater* 33, 33-45.

Brace, W.F., Jones, A.H. [1971] “Comparison of uniaxial deformation in shock and static loading of three rocks,” *J. Geomech. Abstr.* 13(6), 4913–4921.

Cundall, P.A., Strack, O.D.L. [1979] “A discrete numerical model for granular assemblies,” *Geotechnique*, 29, 47-65.

Cusatis, G., Bazant, Z.P. and Cedolin, L. [2003] “Confinement-shear lattice model for concrete damage in tension and compression: 1. Theory,” *J Eng Mech* 129(12), 1439-1448.

Donzé, F.V., Magnier, S.-A., Daudeville, L., Mariotti, C., and Davenne, L. [1999] “Numerical study of compressive behavior of concrete at high strain rates,” *J. Engineering Mechanics* 125 (10), 1154-1163.

Gebbeken, N. [2006] “Residual carrying capacity of structures,” 1st Fraunhofer Sicherheits konferenz Future Security, 4-5 July, Karlsruhe, Germany.

Gong, S. and Lu, Y. [2007] “Combined continua and lumped parameter modelling for nonlinear response of structural frames to impulsive ground shock,” *Journal of Engineering Mechanics* ASCE 133(11), 1229-1240.

Hegemier, G.A. et al. [2002] “FRP-based blast retrofit design strategies – laboratory tests on rectangular RC columns,” Report No. SSRP–2002/04, Department of Structural Engineering, University of California, San Diego, CA.

Hentz, S., Donzé, F.V., and Daudeville, L. [2004] “Discrete Element modeling of concrete submitted to dynamics loading at high strain rates,” *Computers and Structures* 82, 2509-2524.

Hsu, T.T.C., and Zhu, R.R.H. [2002] “Softened membrane model for reinforced concrete elements in shear,” *ACI Structural Journal* 99(4), 460-469.

Krauthammer, T., Assadi-Lamouki, A. and Shanaa, H.M. [1993] “Analysis of impulsive reinforced concrete structural elements - I: Theory,” *Computers and Structures* 48(5), 851-860.

Lellep, J. and Torn, K. [2005] “Shear and bending response of a rigid-plastic beam subjected to impulsive loading,” *Int. J. Impact Engineering* 31, 1081-1105.

Li, Q. M. and Meng, H. [2003] “About the Dynamic strength enhancement of concrete like materials in a split Hopkinson pressure bar test,” *Int J Solids and Structures* 40, 343-360.

Lu, Y. and Tu, Z.G. [2008] “Simulation of concrete fragmentation with a mesoscale approach,” 4th Int. Conf. on Advances in Structural Engineering and Mechanics (ASEM’08), 26-28 May 2008, Jeju, Korea.

Lu, Y. and Wang, Z.Q. [2006] “Characterisation of structural effects from above-ground explosion using coupled numerical simulation,” *Computers and Structures* 84(28), 1729-1742.

Lu, Y., Song, Z.H. and Tu, Z.G [2010] “Analysis of dynamic response of concrete using a mesoscale model incorporating 3D effects,” *Int. J. Protective Structures* 1(2), 197-217.

Lu, Y. and Xu, K. [2004] “Modelling of concrete materials under blast loading,” *Int J Soilds and Structures* 41(1), 131-143.

Ma, G., Shi, H., Shu, D. [2007] “P–I diagram method for combined failure modes of rigid-plastic beams,” *Int J Impact Eng* 34:1081–94.

Malvar, L.J., Crawford, J.E., Wesevich, J.W. [1997] “A plasticity concrete material model for Dyna3D,” *Int. J. Impact Engineering* 19(9-10), 847-873.

Man, K.T., van Mier, J. G. M. [2008] “Size effect on strength and fracture energy for numerical concrete with realistic aggregate shapes,” *Int J Fract* 154, 61–72.

Ross, T. J. [1983] “Direct shear failure in reinforced concrete beams under impulsive loading,” A Dissertation for PH.D., Stanford University.

Park, Y. J., Reinhorn, A. M., and Kunnath, S. K. (1987). IDARC: Inelastic Damage Analysis of Reinforced Concrete Frame-Shear-Wall Structures, Technical Report NCEER-87-0008, State University of New York at Buffalo.

Schlangen, E. and Van Mier, J. G. M., [1992] “Experimental and numerical analysis of micromechanisms of fracture of cement-based composites,” *Cement and Concrete Composites* 14(2), 105-118.

Slawson, T. [1984] “Dynamic shear failure of shallow-buried flat-roofed reinforced concrete structures subjected to blast loading,” Technical Report SL-84-7, Structures Laboratory, U.S. Army Engineer Waterways Experiment Station, Vicksburg, MS.

Song, Z. and Lu, Y. [2010] “An algorithm for generation of 3D mesostructure of concrete for finite element analysis,” 19th UK-ACME Conference, 5-6 April 2011, Edinburgh, UK.

Song, Z. and Lu, Y. [2012] “Mesoscopic analysis of concrete under excessively high strain-rate compression and implications on interpretation of test data,” *International Journal of Impact Engineering* 46, 41–55.

Tu, Z. and Lu, Y. [2011] “Mesoscale modelling of concrete for general FE analysis - Part 1: Model development and implementation,” *Structural Engineering and Mechanics* 37(2), 197-213.

Wang, Z.M., Kwan, A.K.H. and Chan, H.C. [1999] “Mesoscopic study of concrete I: generation of random aggregate structure and finite element mesh,” *Computers and Structures* 70, 533-44.

Wittmann, F.H., Roelfstra, P.E., Sadouki, H. [1984] “Simulation and analysis of composite structures,” *Mater Sci Eng* 68, 239-248.

Wriggers, P. and Moftah, S.O. [2006] “Mesoscale models for concrete: Homogenisation and damage behaviour,” *Finite Elem Anal Des* 42, 623-36.

Xu, K., Lu, Y. [2006] “Numerical simulation study of spallation in reinforced concrete plates subjected to blast loading,” *Computers and Structures* 84(5-6), 431-438.

Zhou, X.Q., Hao, H. [2008] “Mesoscale modelling of concrete tensile failure mechanism at high strain rates,” *Computers and Structures* 86(21-22), 2013–2026.